

*Chapter 2*C-H ACTIVATION MECHANISMS IN NNC AND NCN PINCER
COMPLEXES: A COMPUTATIONAL STUDY

With contributions from Robert J. Nielsen, Meng Zhou, Alan Goldman,
and William A. Goddard III

Some material adapted from:

M. Zhou, M., **S.I. Johnson**, Y. Gao, T.J. Emge, R.J. Nielsen, W.A. Goddard III, A.S. Goldman, Activation and Oxidation of Mesitylene C–H Bonds by (Phebox)Iridium(III) Complexes. *Organometallics*. 2015. 34, 2879–2888

Introduction

Methane co-captured with liquid hydrocarbons in “stranded” (geographically-isolated) wells presents a daunting technical issue. The infrastructure at these wells is tailored to handle liquid products, rather than gaseous methane. In response, this natural gas is typically either flared releasing CO₂ or directly released as methane into the atmosphere. This is environmentally treacherous as both gasses contribute directly to global warming.¹ In response, gas-to-liquid (GTL) technologies have been proposed as a way to efficiently use the methane at hand. Conventional steam-refining of methane (SRM) occurs at temperatures greater than 900 °C, requiring the use of expensive materials for reactors.² The result is that over 65% of the cost of constructing a SRM plant goes to capital costs, making it impractical for use in these stranded wells.² In fact, current GTL technologies are only competitive in cases defined by US Energy Information Administration as “High Oil Price” cases: where oil prices spike to higher than \$200 per barrel.³ Low-cost, low-temperature catalytic conversion of methane to methanol would be the ideal solution in isolated locations since methanol is a liquid at room temperature, making it easy to transport to population centers.⁴ It can be used directly or in a methanol fuel cell.⁴ Previous work towards this goal has been far-reaching, involving a wide variety of metals and ligand platforms.⁵⁻¹¹ Key discoveries include Shilov’s Pt complex, which unfortunately involved irreversible decomposition.¹² Periana’s bipyrimidine Pt complex displayed a high yield, as well as introducing a product protection scheme. In this catalyst, a methyl ester is made rather than methanol. The higher stability of the methyl ester protects the product from over-oxidation.¹³ However, this catalyst also was plagued by decomposition. Efforts to avoid this decomposition included moving to less-electrophilic iridium with the hope of less degradation in the presence

of water. Computational chemistry has been used previously to identify potential iridium-based candidates for catalytic activity¹⁴ as well as to improve existing catalysts. Crucial to improving C-H functionalization catalysts is understanding how existing catalysts function and why they fail to meet turnover frequency and turnover number (TOF and TON, respectively) or selectivity criteria. This involves understanding where potential failure points exist in the mechanism. Gaining this understanding is a strength of computational chemistry, since atomic states along the full potential energy surface can be explored.

Methane oxidation to methanol can be separated into two parts: C-H activation, where the methyl bond is cleaved, and functionalization, where the new functional group is bound to methane. In the case of methanol, this functional group is a hydroxyl group, but other groups can be used in product protection schemes.¹⁵ Two broad modes of C-H activation catalyzed by organometallic iridium have been observed. Heterolytic cleavage of C-H bonds involving Ir^{III} and a coordinated base yields an Ir^{III}-R bond and coordinated “XH.”^{16,17} Alternatively, Ir^V oxo motifs are known to convert alkanes to alcohols without a metal alkyl intermediate. There is evidence that these reactions proceed either via hydrogen atom abstraction and an alkyl radical¹⁸ or via the concerted insertion of a singlet Ir-oxene into the C-H bond.¹⁹

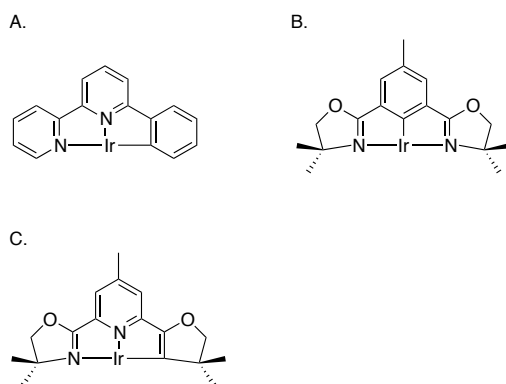


Figure 2.1: a. (NNC)Ir, b. (NCN)Ir (PheBox or NCN) ligand, c. theoretical NCN ligand (*t*NCN)

An organometallic catalyst must be able to activate the strong C-H bonds in methane, resist oxidation by the requisite oxidant to a state inactive toward C-H activation, facilitate the formation of carbon-heteroatom bonds (functionalization) from an Ir-CH₃ intermediate, and react with methane faster than products. Functionalization of methane and alkanes has been

seen in a variety of systems^{13,15,20} and may proceed through either electrophilic attack of the oxidant on the Ir-C bond or by reductive elimination from an oxidation state of Ir higher than Ir^{III}. However, this is out of the scope of the present study.

In this study, two iridium complexes competent for non-radical C-H activation are studied computationally to determine how alterations to their structure can extend their lifetime and activity. Both catalysts are pincer complexes, so modular changes to the structure are feasible, making these systems ideal for study.²¹ (NNC)Ir^{III}(TFA)(C₂H₄)Et (Figure 2.1a, NNC = η^3 -6-phenyl—4,4'-di-tert-butyl-2,2'-bipyridine) catalyzes H/D exchange between 35 atm CH₄ and solvent trifluoroacetic acid (HTFA) at 180 °C with a TOF of 2.12 x 10⁻² s⁻¹. In the presence of 0.4207 mmol oxidant at 180 °C, methane is converted to methyltrifluoroacetate, but the catalyst decomposes on a similar timescale so that a low TON (6.3) is achieved.¹⁵ The NNC framework resulted from a quantum-mechanical rapid prototyping process¹⁴ that screened putative catalysts by activation barriers for H₃C-H activation, redox and M-CH₃ functionalization reactions followed by synthetic elaboration to aid synthesis of the η^3 complex.¹⁵ The second iridium complex, bis(oxazolonyl)phenyl iridium (NCN or Phebox, Figure 2.1b), was shown to dehydrogenate octane²² and catalytically activate benzene and various alkanes in benzene and alkane solvent²³ and has been investigated previously in methane activation.²⁴ These catalysts are named NNC and NCN due to the order in which the terdentate pincer binds to the metal. First, we will investigate experimental results and mechanisms using two monodentate ligands, acetate (OAc) and trifluoroacetate (TFA), in conjunction with the NCN catalyst. In these studies, mesitylene is used as a liquid-phase methane surrogate, as it provides three alkyl sp³ methyl groups for reaction. This study is followed by the comparison between NNC and NCN ligands for C-H activation in methane, as well as predictions for future iterations on this catalyst.

Methods

Geometry optimization, frequency, and solvation calculations were completed using the B3LYP hybrid functional^{25,26} with Los Alamos small core potentials²⁷ and 2- ζ basis set on Ir and 6-31G** on organics.^{28,29} Single point energies were calculated using the M06 functional³⁰ with the LACV3P**++ basis set with augmented *f*-functions and diffuse functions on iridium.³¹ All other atoms were calculated using the 6-311G**++ basis set.^{32,33} Solvation energies in benzene and

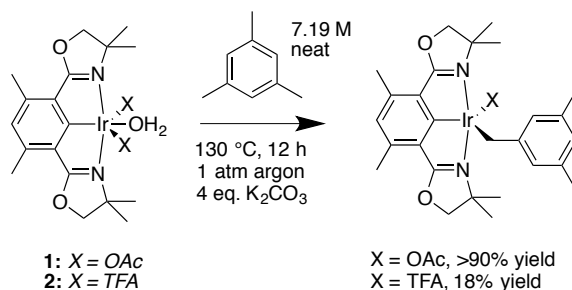
trifluoroacetic acid (TFAH) were calculated using the Poisson-Boltzmann polarizable continuum model. Dielectric constant of 2.238 and probe radius of 2.60 Å were used for solvation in benzene. Free energies of liquid benzene and TFAH were obtained by calculating the 1 atm free energy and subtracting the empirical free energy of vaporization (1.4³⁴ and 1.1³⁵ kcal/mol, respectively). In order to validate transition state geometries, analytical frequency calculations were performed. Free energies were calculated with the following equation:

$$G = E_{M06} + G_{solv} + E_{ZPE} + H_{vib} + H_{TR} - T(S_{vib} + S_{elec})$$

where G_{solv} is the energy of solvation, E_{ZPE} is the zero point energy correction, H_{TR} and S_{TR} are the rotational and translational enthalpy and entropy, and H_{vib} and S_{vib} are the vibrational enthalpy and entropy, respectively. The electronic portion of the entropy is included in the S_{elec} term. The enthalpic and entropic contributions are provided by the frequency calculations. In the case of one-electron and two-electron oxidation, one quarter and one half equivalent of O_2 was used as the oxidant at a potential of 1.2 V vs NHE, respectively. In order to calculate reaction energies involving Ag_2O , DFT calculations were performed using O_2 (1 atm) as oxidant, then corrected using the difference between the standard potentials for the reduction of O_2 to water (1.23 V vs NHE) and $Ag_2O(s)$ to $Ag(s)$ and water (1.17 V vs NHE).³⁶ 1.4 kcal/mol per electron was added to the values obtained using O_2 as the oxidant. Previous studies have shown good agreement between these computational methods and experiment.^{37,38} All calculations were done in Jaguar.³⁹

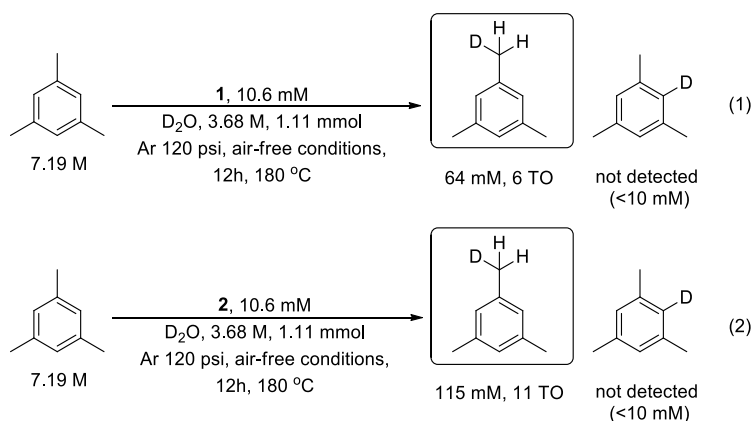
Results and Discussion

Mesitylene Activation and Functionalization by the NCN pincer



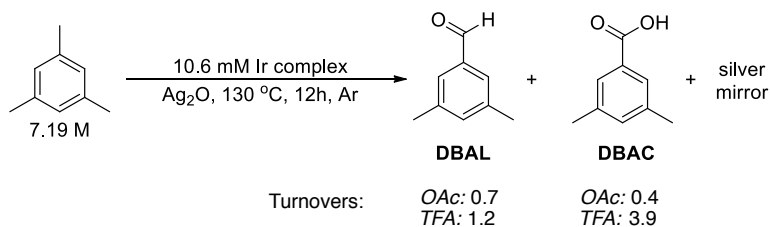
Scheme 2.1: Binding of mesitylene in the (NCN) catalyst shows sensitivity to the X ligand, with X = OAc giving over 90% yield and TFA showing approximately 18% yield.

Experiments were graciously done by Meng Zhou and coworkers at the Goldman Group of Rutgers University. Relevant results are summarized here, but for full experimental details, the reader is referred to the corresponding paper.⁴⁰ Scheme 2.1 shows the results of C-H activation of the sp^3 hybridized carbon of mesitylene by the aquo analogue of NCN with 4 equivalents of K_2CO_3 at elevated temperatures. While the mechanism for this reaction will be discussed *vide infra*, it can be assumed that the X ligand is lost as HX. The OAc complex (**1**) shows 90% yield of the bound mesitylene group; however, the TFA analogue (**2**) only shows 18% yield.



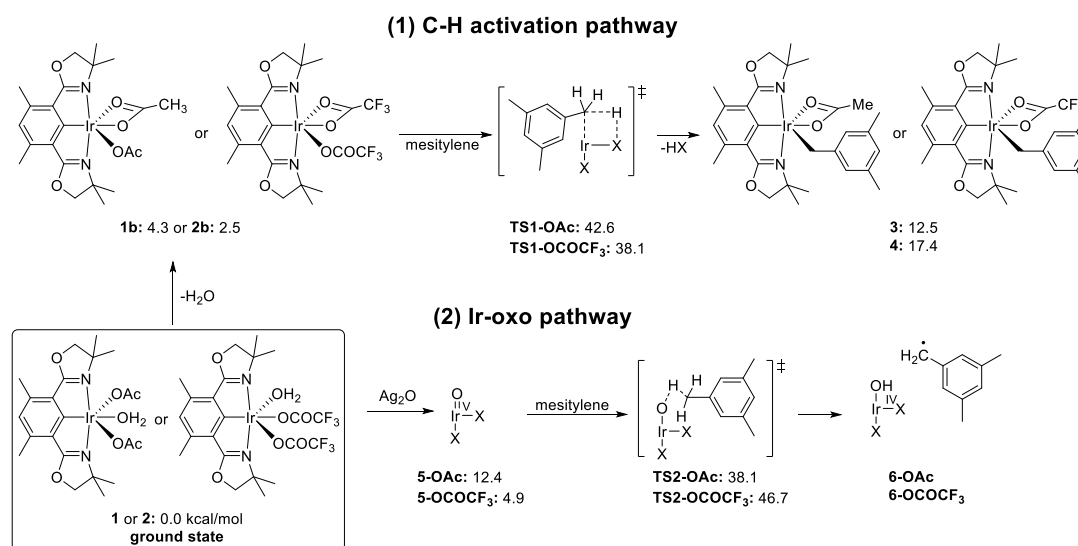
Scheme 2.2: Results of H/D exchange reactions, showing that the TFA analogue undergoes approximately twice as many turnovers as the OAc analogue.

Despite the lower yield of the bound mesitylene complex, the **2** ligand (TFA) shows nearly twice as many turnovers in H/D exchange experiments than **1** (OAc) in D_2O at elevated temperatures (Scheme 2.2). No benzylic H/D exchange was detected within the limits of the experiments. This result implies that at some point even in the TFA complexes, mesitylene is bound to the Ir center.



Scheme 2.3: Ratios of aldehyde (DBAL) to carboxylic acid (DBAC) product for the OAc and TFA analogues.

The reaction shown in Scheme 2.3 further corroborates mesitylene is bound at some point. In both cases 3,5-dimethylbenzaldehyde (**DBAL**) and 3,5-dimethylbenzoic acid (**DBAC**) are formed in differing ratios. In **1**, more aldehyde than carboxylic acid is formed, implying that less over-oxidation occurs. However, there is only 1.1 turnover of total product formed. In the case of **2**, three times the DBAC is formed than DBAL, implying more over-oxidation. However, multiple turnovers of product are formed. In order to improve this catalysts ability to functionalize mesitylene (as a first step to understanding methane oxidation), a computational mechanistic search was undertaken.



Scheme 2.4. Calculated free energies (kcal/mol) for (1) C-H activation pathway and (2) Ir-oxo pathway in catalytic mesitylene oxidation using complexes **1** or **2**; X = OAc or OCOCF₃; “Phebox” ligand was not shown but was implied, except in complexes **1**, **2**, **3**, and **4**; no calculations performed for **6-OAc** and **6-OCOCF₃**

Two proposed pathways for mesitylene C-H bond activation by complexes **1** and **2** are shown in Scheme 2.4. The experimentally prepared aquo complexes were taken as the ground states for all calculations. Two different ground states were calculated for the two coordinating ligands. In complex **1**, the ground state for the acetate complex, the coordinated aquo ligand prefers to occupy the equatorial position, whereas in complex **2**, the ground state for the trifluoroacetate complex, the aquo ligand prefers the axial position. In pathway (1), C-H activation of mesitylene

proceeds *via* **TS1** with binding of the benzylic carbon to iridium occurring concertedly with hydrogen transfer to the oxygen of the anionic ligand (a concerted metalation-deprotonation or CMD mechanism).^{36,41,42}

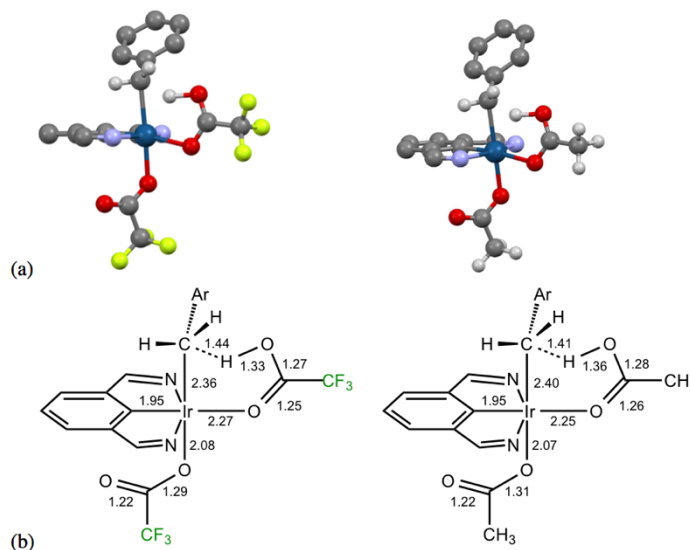


Figure 2.2: (a) Calculated structure of TS1-OCOCF₃ and TS1-OCOCH₃ (peripheral atoms omitted for clarity) (b) Selected interatomic distances indicated (Å)

In C-H activation by complex **1**, the transition state **TS1-OAc** has an activation barrier of 42.6 kcal/mol. The trifluoroacetate analog, **TS1-OCOCF₃** (Fig. 2.2), is lower in free energy, 38.1 kcal/mol. Proceeding along the reaction coordinate from **TS1**, the acetic acid or trifluoroacetic acid (HX) molecule is eliminated to give complex **3** or **4**. Notably, although **TS1-OAc** has a higher energy than **TS1-OCOCF₃**, formation of the reaction product, **3** (from **TS1-OAc**), is significantly less endergonic than formation of complex **4** (from **TS1-OCOCF₃**) (by 6.2 kcal/mol). These transition states and relevant bond lengths can be seen in Figure 2.2. Thus the calculations are consistent with both the faster kinetics of H/D exchange catalyzed by **2** vs. **1**, and the observations indicating that C-H activation by **2** to give the mesityl complex **4** is thermodynamically less favorable than the reaction of **1** to give **3**. It should be noted however that the calculated differences in both the reaction kinetics and thermodynamics are much greater than is indicated by the experimental results.

Once formed, complexes **3** or **4** may undergo a variety of possible routes discussed in the literature to form a C-O bond;^{43,44} the complexity of such reactions, particularly with Ag₂O as oxidant, is beyond the scope of this work. An alternative oxidation pathway begins with the direct oxidation to give Ir-oxo complexes **5**. Iron, manganese, and ruthenium oxo complexes typically can undergo a fast hydrogen abstraction reaction with alkanes, often leading to over-oxidation.^{45,46} This reaction yields a carboradical and Ir^{IV} hydroxide complex, shown in **6**. The formation of **5-OAc** is uphill from **1** by 12.4 kcal/mol, while the formation of **5-OCOCF₃** is only uphill from **2** by 4.9 kcal/mol.

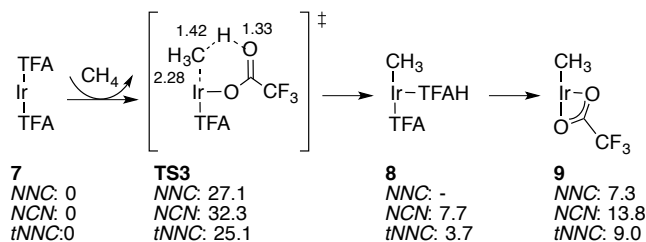
The transition state for hydrogen abstraction by the oxo group is shown by **TS2**. At 38.1 kcal/mol, the calculated barrier for hydrogen abstraction by Ir-oxo complex **5-OAc**, *via* transition state **TS2-OAc**, is lower than **TS2-OCOCF₃** (46.7 kcal/mol), by 8.6 kcal/mol. Given that the trifluoroacetate complex **2** is the more effective catalyst for oxidation, and given that a calculated comparison of two such closely analogous transition states should be quite reliable, this argues strongly against the oxo pathway (at least for catalysis by complex **2**). In marked contrast, for the C-H activation pathway, **TS1-OCOCF₃** is significantly lower than **TS1-OAc**, in accord with the observation that complex trifluoroacetate complex **2** catalyzes both oxidation and H/D exchange faster than complex **1**.

Thus the calculations predict that the trifluoroacetate ligand favors the kinetics of C-H activation (in accord with the faster H/D exchange) as compared with the acetate ligand, while it disfavors the oxo pathway. This may suggest that trifluoroacetate in this type of system is more promising than acetate for C-H functionalization, since the oxo pathway (if operative) is less likely to afford the intriguing selectivity that is offered by transition-metal catalyzed C-H activation.⁴⁵ As such, all further comparison will be using TFA as the monodentate ligand.

Comparison of NNC and NCN pincer systems

Free energy surfaces for the heterolytic activation of methane by both the NNC and NCN catalysts are seen in Scheme 2.5. The mechanism proceeds by the non-aquo complex **7**, concertedly transferring a proton from methane to coordinated trifluoroacetate and binding carbon to iridium in the CMD scheme, as shown by **TS3**. The protonated TFA is then released by the catalyst and the remaining TFA forms a κ^2 bond to the iridium to form **9**. The structure

for **9** has been observed experimentally in benzene and alkane activation by Ito et al.²³, supporting this mechanism. Comparing the transition state and intermediate energies, the NNC catalyst has a lower activation barrier of 27.1 kcal/mol, lower when compared to the NCN catalyst, which has an activation barrier of 32.3 kcal/mol. Both of these activation energies are accessible in the temperatures used for methane activation. The free energy for **9** is similarly higher in the NCN catalyst than the NNC catalyst, suggesting it may be difficult to isolate.⁴⁰

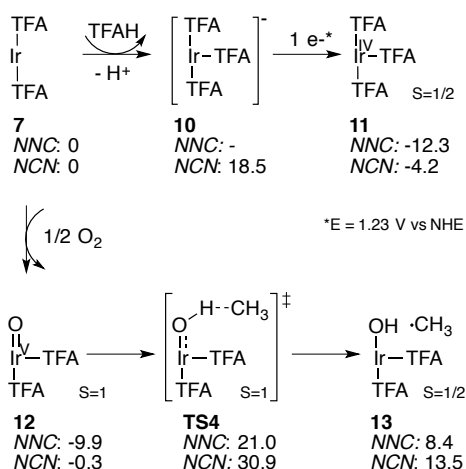


Scheme 2.5: Methane activation occurs in this scheme by concerted metalation/deprotonation. Due to the decreased *trans* influence, the NNC complex yields the lowest barrier.

A problem that has plagued these catalysts is the formation of an oxidized, deactivated Ir^{IV} state⁴⁶, which features three bound TFA molecules as seen in Scheme 2.6. The free energies of the Ir^{IV} intermediates **11** are calculated using O₂ as an oxidant. The NNC catalyst forms **11**^{NNC} quite easily, as it is downhill from the resting state **7** by 12.3 kcal/mol. This suggests that this state provides a thermodynamic sink. In contrast, **11**^{NCN} is downhill by 4.2 kcal/mol from the resting state, but is less exergonic than the NNC ligand. In this sense, the NCN catalyst performs better in that it is more resistant to oxidation by one electron over a wider range of oxidation potentials, as seen experimentally, though is still exergonic to form.⁴⁰ In fact, this state may be one reason for the limited turnovers for Phebox in the previously-described mesitylene activation and functionalization.

Another undesired reaction that can occur is the formation of an Ir^V oxo, which can then participate in hydrogen atom transfer (HAT) reactions. Radical activation is undesirable because it is typically unselective among C-H bonds and can therefore lead to over-oxidation to CO₂.⁴⁵ This reaction should be avoided if the goal is selective oxidation of methane. The free energy surface for radical fast hydrogen transfer can be seen in Scheme 2.6. After the Ir^V-oxo, **12**, is formed, methane transfers a hydrogen through a radical mechanism to the oxygen, yielding an

iridium hydroxide complex and a radical methyl group. The methyl group then quickly bonds with the hydroxide. In the NNC catalyst, the oxo represents a potential resting state for the system, as formation is still exergonic by -9.9 kcal/mol, whereas the NCN oxo complex is thermally neutral with the previous ground state **7**. The transition state barrier, **TS4**, is uphill 21 kcal/mol for the NNC catalyst from **7**^{NNC}, and is uphill by 30.9 kcal/mol from the new assumed resting state of **12**^{NNC}. In the NCN system, **TS4**^{NCN} is uphill 30.9 and 31.2 kcal/mol from states **7** and **12**, respectively. From their respective resting states, the NNC and NCN systems have similar HAT barriers. These barriers are also competitive with **TS3**, suggesting oxidation may be a competitive process in non-radical methane activation.

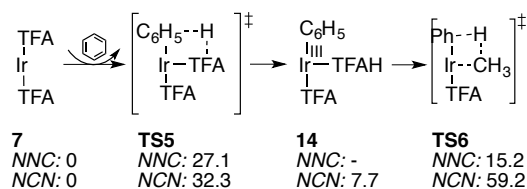


Scheme 2.6: Two undesired pathways are shown. The top pathway displays the deactivated Ir^{IV} complex and the lower pathway shows the formation of the iridium oxo complex.

The barrier for formation of the oxo is not calculated. This barrier is assumed to be quick due to work by Brown et al⁴⁷, which proposed a bimolecular reaction in trimesityliridium, where two iridiums bond with dioxygen, cleaving the bond. This mechanism is supported kinetically by second order reaction rates with respect to iridium. No intermediate has been seen, which suggests that this reaction proceeds quickly.⁴⁷ If this is the case, then the formation of **TS3** is the rate-limiting step and the energies of **12** are indicative of the tendency to proceed through the radical pathway.

In benzene, phenyl activation can occur as a competing reaction. Alternatively, the activation of benzene could provide a mediated pathway that lowers the activation barrier for methane, as

can be seen in Scheme 2.7. In this mechanism, benzene is first activated in a manner similar to methane. Subsequently, methane transfers a hydrogen to the phenyl group, which is released. The methyl group then binds to iridium. In both the NNC and NCN catalysts, the barrier for activation of benzene is lower than that of methane. Additionally, the intermediate analogous to **9** is seen experimentally in the NCN catalyst²³, which provides experimental evidence for the proposed computational mechanism. The hydrogen transfer step, **TS6**, is low in energy for the NNC catalysts at 15.2 kcal/mol and is thermally accessible. However, in the NCN catalyst, the transfer is much too high in energy (59.2 kcal/mol in benzene) for the reaction to be thermally feasible. Since the phenyl-activated intermediate is seen experimentally in NCN, this may be a competing reaction. This highlights the importance of solvent choice in catalysis: choosing another solvent such as TFAH⁶ or halogenated benzene ameliorates this problem.



Scheme 2.7: Activation of benzene is competitive with methane activation in both the NNC and NCN, as shown by **TS5**.

Significant differences can be seen between the pathways available to the NNC and NCN pincers. These differences can be attributed to the position of the carbon in the pincer. In the NCN case, the carbon competes for the orbital with the atoms directly across from it, frustrating bonding in the equatorial position. In the NNC system, nitrogen in the pyridine ring is less effective as a donor⁴⁸, which affects the bonding of relevant methyl and TFA molecules less. This can be seen explicitly if we examine an NNC analog of Phebox, which can be seen in Figure 2.1c. This theoretical molecule is obtained by switching the position of the carbon in the pincer, but retaining the rest of the Phebox structure. Activation of methane using this theoretical pincer molecule follows the same motif as in Scheme 2.1, where it is referred to as tNNC. However, the tNNC analog has a lower free energy for molecules **9** and **11** than its NCN analog, which is to be expected based off the current hypothesis. This also agrees with other work investigating nitrogen groups in the *ipso* position to the metal.²⁴ When comparing the formation of the Ir^{IV} deactivated complex **7**, the tNNC forms it favorably (-18.9 kcal/mol) as expected. When

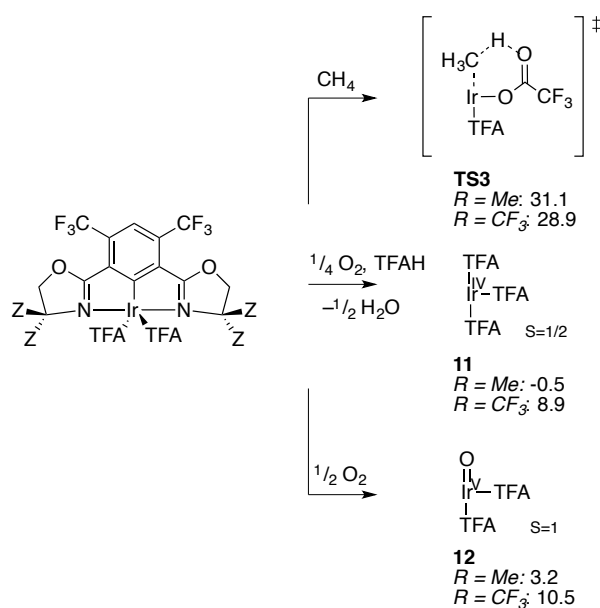
comparing bond lengths between the iridium and the oxygen of the equatorial TFA in **7**, the original NNC molecule has a length of 2.16 Å, while the tNNC molecule forms a shorter bond length of 2.07 Å. The increased bond length when C is *trans* to the TFA is expected because competition for the orbital is a determining factor in the behavior of Phebox as a catalyst.

The strong influence of the *trans* effect explains much of the other observed behavior of the NNC catalyst. In the phenyl-mediated activation pathway **TS6**, the two carbons *trans* to one another frustrate the molecule, leading to an increased transition state energy. It also increases the energy **11**: having three TFA groups bound to the iridium is unfavorable because one of the TFAs must reside opposite the C-Ir bond. Finally, the effect is also seen in the ground state. In the NNC system and in other molecules the TFA will form a κ^2 bond with the Ir. However, in the NCN system, the bond with the TFA group is only to a single oxygen, or κ^1 , despite their orientations being similar. This suggests again the important effect that the carbon in the pincer has on the position *trans* to it.

With this information about the importance of the *ipso* carbon in hand, the pincer can be modified in order to lower the barrier for CMD (**TS3**), while raising the energy of undesired intermediates **11** and **12**. Increased competition for the orbital shared by the *ipso* carbon and the equatorial position disfavors undesired states; increased electron density in this position may improve performance. Directing groups on the phenyl backbone can be used in order to achieve this goal. For example, CF₃ groups are *meta*-directing,⁴⁹ so hypothetically these groups could be used to modify electron density at the *ipso* carbon if cleverly placed. Computational results of this prediction can be seen in Scheme 2.8.

Upon adding CF₃ groups to the *meta* positions of the pincer (CH₃ groups in the Z groups), the barrier for CMD is lowered by approximately 1 kcal/mol, a negligible amount. More promising, however, is the increase in energy of intermediates **11** and **12**. Whereas in the unmodified example, the formation of the deactivated complex **11** was exergonic (-4.2 kcal/mol), but with appropriate CF₃ groups is now thermoneutral. Complex **12** is also more endergonic to form. The situation can further be improved by using R = CF₃ in addition the CF₃ *meta* substitution, fully trifluoromethylating the catalyst. The barrier for **TS3** is further decreased to 28.9 kcal/mol, and the energy for **11** and **12** now significantly endergonic. The effect of the Z group can be attributed to the electron withdrawing nature of CF₃ groups⁵⁰, as it removes electron

density from the Ir center and gently tunes the catalyst to be slightly more electrophilic. This could potentially hit a sweet spot between the less electrophilic, non-fluorinated Ir complex and the more electrophilic noble metals previously used.¹² Additionally, the CF₃ groups may have an electrostatic effect, as they may repel the oxygen of TFA, making it more difficult to coordinate.⁵¹ While Ir complexes with *meta*-CF₃ groups^{52,53} and Z = CF₃ groups⁵¹ have been made independently, a complex with full trifluoromethylation may be synthetically difficult to produce. However, the above mechanistic study suggests that efforts toward these molecules could yield a very interesting catalyst and should be pursued.



Scheme 2.8: Use of electron withdrawing group CF₃ aids in lowering the barrier for CMD while also raising the energy of undesired intermediates leading to deactivation and side reactions.

Conclusions

While the activation energy of the NNC catalyst is lower than that of NCN catalyst, the characteristics of the NCN Phebox pincer help it avoid some of the pitfalls that had previously plagued the NNC catalyst, including oxidation. However, Phebox has its own pitfalls, including an inability to transfer hydrogen between a phenyl group and methyl group, making phenyl activation a competing reaction rather than a helpful one when the catalysis is performed in benzene. Steps to avoid the formation of **12** and bias the reaction towards a non-radical pathway can be taken, including using a different oxidant and using ligand modifications presented here.

Another route is to investigate PCP ligands, which have been shown to avoid the Ir^V state.⁵⁴

The overarching goal is to protect these iridium catalysts from over-oxidation, while maintaining high turnover numbers. The fluorinated complexes are a potential improvement in this direction, but more work should be done to understand their ability to catalyze methane oxidation. Future work largely involves understanding functionalization better and applying this to the fluorinated ligand sets. Additionally, more reasonable oxidants than Ag₂O, or even oxygen, should be considered, both for experiment and calculational work. Nonetheless, the interesting characteristics of Phebox and its fluorinated derivatives make it a potential candidate for use in methane activation.

References

- (1) Lashof, D. A.; Ahuja, D. R. *Nature* **1990**, *344*, 529-531.
- (2) Aresta, M. *Carbon Dioxide Reduction and Uses as a Chemical Feedstock*; Wiley-VCH: Weinheim, Germany, 2006.
- (3) EIA; Energy, D. o., Ed. Washington DC, 2016.
- (4) Olah, G. A. *Angew. Chem. Int. Ed.* **2013**, *52*, 104-107.
- (5) Tenn, W. J.; Young, K. J. H.; Bhalla, G.; Oxgaard, J.; Goddard, W. A.; Periana, R. A. *J. Am. Chem. Soc.* **2005**, *127*, 14172-14173.
- (6) Ahlquist, M.; Periana, R. A.; Goddard Iii, W. A. *Chem. Comm.* **2009**, 2373-2375.
- (7) Cheng, M.-J.; Bischof, S. M.; Nielsen, R. J.; Goddard Iii, W. A.; Gunnoe, T. B.; Periana, R. A. *Dalton T.* **2012**, *41*, 3758-3763.
- (8) Crabtree, R. H. *J. Organomet. Chem* **2004**, *689*, 4083-4091.
- (9) Stahl, S. S.; Labinger, J. A.; Bercaw, J. E. *J. Am. Chem. Soc.* **1996**, *118*, 5961-5976.
- (10) Hashiguchi, B. G.; Bischof, S. M.; Konnick, M. M.; Periana, R. A. *Acc. Chem. Res.* **2012**, *45*, 885-898.
- (11) Periana, R. A.; Mironov, O.; Taube, D.; Bhalla, G.; Jones, C. *Science* **2003**, *301*, 814-818.
- (12) Shilov, A. E. *Activation of Saturated Hydrocarbons by Transition Metal Complexes*; Reidel: Dordrecht, Netherlands, 1984.
- (13) Periana, R. A.; Taube, D. J.; Gamble, S.; Taube, H.; Satoh, T.; Fujii, H. *Science* **1998**, *280*, 560.
- (14) Muller, R. P.; Philipp, D. M.; Goddard, W. A., III *Top. Catal.* **2003**, *23*, 81-98.
- (15) Young, K. J. H.; Oxgaard, J.; Ess, D. H.; Meier, S. K.; Stewart, T.; Goddard, I. I. I. W. A.; Periana, R. A. *Chem. Comm.* **2009**, *0*, 3270-3272.
- (16) Davies, D. L.; Donald, S. M. A.; Al-Duaij, O.; Macgregor, S. A.; Pölleth, M. J. *Am. Chem. Soc.* **2006**, *128*, 4210-4211.
- (17) Ess, D. H.; Nielsen, R. J.; Goddard Iii, W. A.; Periana, R. A. *J. Am. Chem. Soc.* **2009**, *131*, 11686-11688.
- (18) Groves, J. T. *J. Chem. Educ.* **1985**, *62*, 928.
- (19) Zhou, M.; Balcells, D.; Parent, A. R.; Crabtree, R. H.; Eisenstein, O. *ACS Catal.* **2011**, *2*, 208-218.
- (20) Conley, B. L.; Ganesh, S. K.; Gonzales, J. M.; Tenn, W. J.; Young, K. J. H.; Oxgaard, J.; Goddard, W. A.; Periana, R. A. *J. Am. Chem. Soc.* **2006**, *128*, 9018-9019.
- (21) Albrecht, M.; van Koten, G. *Angew. Chem. Int. Ed.* **2001**, *40*, 3750-3781.
- (22) Allen, K. E.; Heinekey, D. M.; Goldman, A. S.; Goldberg, K. I. *Organometallics* **2013**, *32*, 1579-1582.
- (23) Ito, J.-i.; Kaneda, T.; Nishiyama, H. *Organometallics* **2012**, *31*, 4442-4449.
- (24) Pahls, D. R.; Allen, K. E.; Goldberg, K. I.; Cundari, T. R. *Organometallics* **2014**, *33*, 6413-6419.
- (25) Becke, A. D. *J. Chem. Phys.* **1993**, *98*, 5648-5652.
- (26) Lee, C. T.; Yang, W. T.; Parr, R. G. *Phys. Rev. B* **1988**, *37*, 785-789.
- (27) Hay, P. J.; Wadt, W. R. *J. Chem. Phys.* **1985**, *82*, 299-310.
- (28) Francl, M. M.; Pietro, W. J.; Hehre, W. J.; Binkley, J. S.; Gordon, M. S.; Defrees, D. J.; Pople, J. A. *J. Chem. Phys.* **1982**, *77*, 3654-3665.
- (29) Hehre, W. J.; Ditchfie.R; Pople, J. A. *J. Chem. Phys.* **1972**, *56*, 2257-2261.
- (30) Zhao, Y.; Truhlar, D. G. *Theor. Chem. Acc.* **2008**, *120*, 215-241.
- (31) Martin, J. M. L.; Sundermann, A. *J. Chem. Phys.* **2001**, *114*, 3408-3420.
- (32) Krishnan, R.; Binkley, J. S.; Seeger, R.; Pople, J. A. *J. Chem. Phys.* **1980**, *72*, 650-654.
- (33) Clark, T.; Chandrasekhar, J.; Spitznagel, G. W.; Schleyer, P. V. *J. Comp. Chem.* **1983**, *4*, 294-301.
- (34) Deshpande, D. D., Pandya M.V., *Trans. Faraday Soc.* **1967**, *63*, 2149-2157.
- (35) Kreglewski, A. *Bull. Acad. Pol. Sci. Ser. Sci Chim.* **1962**, *10*, 629-633.
- (36) Pourbaix, M.; Gauthier Villars Paris, 1963.
- (37) Zhao, Y.; Truhlar, D. G. *J. Chem. Theory Comp.* **2009**, *5*, 324-333.
- (38) Young, K. J. H.; Lokare, K. S.; Leung, C. H.; Cheng, M.-J.; Nielsen, R. J.; Petasis, N. A.; Goddard III, W. A.; Periana, R. A. *J. Mol. Catal. A: Chem.* **2011**, *339*, 17-23.
- (39) Bochevarov, A. D.; Harder, E.; Hughes, T. F.; Greenwood, J. R.; Braden, D. A.; Philipp, D. M.; Rinaldo, D.; Halls, M. D.; Zhang, J.; Friesner, R. A. *Int. J. Quantum Chem.* **2013**, *113*, 2110-2142.
- (40) Zhou, M.; Johnson, S. I.; Gao, Y.; Emge, T. J.; Nielsen, R. J.; Goddard, W. A.; Goldman, A. S. *Organometallics* **2015**, *34*, 2879-2888.
- (41) Jones, C. J.; Taube, D.; Ziatdinov, V. R.; Periana, R. A.; Nielsen, R. J.; Oxgaard, J.; Goddard, W. A. *Angewandte Chemie International Edition* **2004**, *43*, 4626-4629.
- (42) Lapointe, D.; Fagnou, K. *Chem. Lett.* **2010**, *39*, 1118-1126.

- (43) Conley, B. L.; Tenn, W. J.; Young, K. J. H.; Ganesh, S. K.; Meier, S. K.; Ziatdinov, V. R.; Mironov, O.; Oxgaard, J.; Gonzales, J.; Goddard, W. A.; Periana, R. A. *J. Mol. Catal. A: Chem.* **2006**, *251*, 8-23.
- (44) Young, K. J. H.; Oxgaard, J.; Ess, D. H.; Meier, S. K.; Stewart, T.; Goddard, I. I. I. W. A.; Periana, R. A. *Chem. Comm.* **2009**, 3270-3272.
- (45) Labinger, J. A. *Catal. Lett.* **1988**, *1*, 371-375.
- (46) Fu, R.; Bercaw, J. E.; Labinger, J. A. *Organometallics* **2011**, *30*, 6751-6765.
- (47) Jacobi, B. G.; Laitar, D. S.; Pu, L.; Wargocki, M. F.; DiPasquale, A. G.; Fortner, K. C.; Schuck, S. M.; Brown, S. N. *Inorg. Chem.* **2002**, *41*, 4815-4823.
- (48) Wang, D. Y.; Choliy, Y.; Haibach, M. C.; Hartwig, J. F.; Krogh-Jespersen, K.; Goldman, A. S. *J. Am. Chem. Soc.* **2016**, *138*, 149-163.
- (49) Carey, F. A. *Organic Chemistry*; 7th ed., 2007.
- (50) Hansch, C.; Leo, A.; Taft, R. W. *Chem. Rev.* **1991**, *91*, 165-195.
- (51) Roddick, D. M. In *Organometallic Pincer Chemistry*; van Koten, G., Milstein, D., Eds.; Springer Berlin Heidelberg: Berlin, Heidelberg, 2013, p 49-88.
- (52) Cai, J.-G.; Yu, Z.-T.; Yuan, Y.-J.; Li, F.; Zou, Z.-G. *ACS Catal.* **2014**, *4*, 1953-1963.
- (53) Brulatti, P.; Gildea, R. J.; Howard, J. A. K.; Fattori, V.; Cocchi, M.; Williams, J. A. G. *Inorg. Chem.* **2012**, *51*, 3813-3826.
- (54) Adams, J. J.; Lau, A.; Arulsamy, N.; Roddick, D. M. *Organometallics* **2011**, *30*, 689-696.